The Canadian Mineralogist
Vol. 37, pp. 1405-1421 (1999)

PARAGENESIS AND COMPOSITION OF AMPHIBOLE AND BIOTITE IN THE MacLELLAN GOLD DEPOSIT, LYNN LAKE GREENSTONE BELT, MANITOBA, CANADA

IAIN M. SAMSON[1], WILLIAM H. BLACKBURN[2] AND JOEL E. GAGNON[3]

Department of Earth Sciences, University of Windsor, Windsor, Ontario N9B 3P4, Canada

Abstract

The Proterozoic MacLellan gold deposit, in the Lynn Lake greenstone belt, Manitoba, developed through a complex sequence of pre-, syn- and postmetamorphic fluid-infiltration events within a series of amphibolite-grade biotite-, chlorite- and amphibole-bearing schists. Amphibole within the deposit is manifested as a wide variety of textural types, including metamorphic porphyroblasts, randomly oriented postmetamorphic porphyroblasts and aggregates, amphiboles related to quartz – chlorite – biotite vugs, and aggregates of massive amphibole in alteration haloes around veins. The amphiboles are all calcic, but represent a wide compositional range, and includes the varieties ferrotschermakite, tschermakite, magnesiohornblende and actinolite. Distribution of Fe and Mg among amphibole, biotite and chlorite indicate three amphibole-forming events, which represent 1) metamorphism, 2) the main quartz–amphibole vein-forming and alteration event, and 3) an event that formed the vugs. The randomly oriented porphyroblasts and aggregates appear to be associated with both the main alteration event and the vug-forming event, which is consistent with their formation after the main episode of metamorphism and deformation. The chemical composition of the protolith strongly influenced the composition of alteration amphiboles. Alteration occurred under low water:rock ratios. Biotite, the other main mafic mineral, is generally Mg-rich. The composition of biotite in and around metamorphosed quartz – biotite – sulfide (QBS) veins is more restricted than that of the host-rock biotite, which suggests that these compositions represent a fluid-buffered protolith composition. Titanium contents of the biotite correlate with the nature of the associated Ti-oxide phase, increasing from rutile to ilmenite ± rutile to titanite – ilmenite ± rutile. The QBS-associated biotite typically has a high Ti content and is associated with titanite. This assocation may well result from premetamorphic metasomatism related to the QBS vein-forming event.

Keywords: amphibole, biotite, mineral composition, gold, MacLellan deposit, paragenesis, hydrothermal, Lynn Lake greenstone belt, Manitoba.

Sommaire

Le gisement d'or MacLellan, d'âge protérozoïque, situé dans la ceiture de roches vertes du lac Lynn, au Manitoba, s'est développé suite à une séquence complexe d'événements pré-, syn- et postmétamorphiques impliquant une infiltration de fluide dans une série de schistes à biotite, chlorite et amphibole équilibrés aux conditions du faciès amphibolite. L'amphibole du gisement se présente sous une grande variété de textures, y inclus porphyroblastes synmétamorphiques, d'autres dont l'orientation est aléatoire et qui seraient postmétamorphiques, en partie en aggrégats, de l'amphibole liée aux cavités tapissées de quartz – chlorite – biotite, et des aggrégats d'amphibole massive dans les auréoles d'altération longeant les veines. Les amphiboles sont toutes calciques, mais elle représentent une grande étendue de compositions et donc de variétés, dont ferrotschermakite, tschermakite, magnésiohornblende et actinolite. La distribution de Fe et de Mg parmi amphibole, biotite et chlorite coexistantes indique trois épisodes de formation: 1) métamorphisme, 2) événement principal de formation des veines d'amphibole et de quartz, et d'altération, et 3) formation des cavités. Les porphyroblastes à orientation aléatoire et les aggrégats semblent être associés à la fois à l'épisode principal d'altération et la formation des cavités, ce qui concorde avec leur déroulement après la recristallisation métamorphique principale et la recristallisation. La composition chimique du protolithe a fortement influencé la composition des amphiboles des assemblages d'altération. L'altération se caractérise donc par un faible rapport de roche à H_2O. La biotite, l'autre phase mafique importante, est en général magnésienne. Sa composition dans et près des veines métamorphisées à quartz – biotite – sulfures est plus restreinte que celle des roches-hôtes, ce qui fait penser qu'elles résultent d'un protolithe dont la composition était régie par la composition du fluide. La teneur en titane de la biotite montre une corrélation avec la nature de l'oxyde coexistant porteur de Ti, augmentant à partir de rutile à ilménite ± rutile à titanite – ilménite ± rutile. La biotite des veines à sulfures possède en général une teneur élevée en Ti et coexiste avec la titanite. Cette assocation pourrait bien résulter d'une métasomatose pré-métamorphique liée à la formation des veines sulfurées.

(Traduit par la Rédaction)

Keywords: amphibole, biotite, composition des minéraux, or, gisement MacLellan, paragenèse, hydrothermal, ceinture de roches vertes du lac Lynn, Manitoba.

[§] *E-mail address*: ims@uwindsor.ca
[2] Present address: Royal Roads University, Victoria, British Columbia V9B 5Y2, Canada.
[3] Present address: Atwell-Hicks, Inc., 540 Avis Drive, Ann Arbor, Michigan 48108, U.S.A.

Introduction

The MacLellan gold deposit occurs within a sequence of mineralogically diverse amphibolite-grade schists in a predominantly metavolcanic portion of the Lynn Lake greenstone belt in Manitoba. The deposit contains at least four distinct sets of veins, the timing of which ranges from premetamorphic to postmetamorphic (Samson & Gagnon 1995). Biotite and amphibole are abundant both in the host rocks and in vein and alteration assemblages. In this paper, we focus on the paragenesis of the various types of biotite and amphibole, and use data on the composition of these mafic minerals to examine the genetic relationships among biotite, amphibole and chlorite in this complex deposit, particularly with respect to metamorphism and fluid infiltration.

Geology

The MacLellan gold deposit is located approximately 8 km northeast of Lynn Lake, Manitoba (Fig. 1), and is hosted by amphibolite-grade schists that form part of the Wasekwan Group of the Paleoproterozoic Lynn Lake greenstone belt (Gilbert *et al.* 1980, Fedikow 1986, Samson & Gagnon 1995). The deposit is one of three mineralized bodies that form a zone of mineralization crudely stratiform and subconcordant to the enclosing stratigraphy (Fedikow *et al.* 1991, Samson & Gagnon 1995). In the vicinity of the mine, chlorite- and amphibole-rich schists that have been interpreted as metamorphosed aluminous and picritic metabasalts dominate the Wasekwan Group (Gagnon 1991, Fedikow 1992). Subordinate biotite- and quartz-rich schist units have been variously interpreted as pyroclastic and epiclastic units (Fedikow 1992).

Most of the samples used in this study came from the main conveyor drift on the 370 m level of the MacLellan mine; the drift was mapped at a scale of 1:100 (Gagnon 1991, Samson & Gagnon 1995) and provided a complete cross-section through the deposit. A few additional samples came from an active stope, spoil heaps and surface exposures.

Host Rocks

In order of decreasing abundance, the rocks hosting the mineralization are chlorite – hornblende (CH) schist, biotite – plagioclase (BP) schist, and chlorite – quartz (CQ) schist (Gagnon 1991, Samson & Gagnon 1995). Few primary structures or textures are recognizable. These assemblages and individual samples can be very heterogeneous, with millimeter- to centimeter-scale banding of mineralogically diverse rock-types. CH schists consist of amphibole, chlorite and plagioclase with accessory magnetite, ilmenite and epidote. CQ schists principally consist of quartz, chlorite, plagioclase and biotite with minor amphibole, garnet, magnetite and ilmenite. BP schists are the most heterogeneous host-rocks. In addition to the dominant plagioclase, biotite and chlorite, these rocks may contain minor ilmenite, magnetite, rutile, titanite, alkali feldspar, epidote, kyanite, amphibole, quartz, staurolite, garnet, tourmaline, pyrite and pyrrhotite. Biotite within the host BP schists is light brown and, in general, fine-grained. Staurolite typically occurs as porphyroblasts that grew at the expense of biotite. Titanite occurs as rims around ilmenite and rutile crystals. Quartz–muscovite schist is a rare rock-type in the sequence. The grade of metamorphism in the vicinity of the deposit ranges from lower to middle amphibolite facies (Gilbert *et al.* 1980), which is consistent with the presence of garnet, staurolite and rare kyanite in the biotite schists (Samson & Gagnon 1995). Most samples of the schists have a single, penetrative foliation. Rare crenulation cleavage is related to narrow, late-kinematic shear zones (Gagnon 1991, Samson and Gagnon 1995).

Amphibole within the schists is optically and texturally variable (Table 1, Figs. 2, 3, and 4). In some schists, fine- to medium-grained, subidioblastic to idioblastic crystals of amphibole show a preferred orientation that is conformable with the penetrative foliation defined by matrix chlorite and biotite (referred to as "metamorphic" in Table 1). In most samples, however, many or all of the amphibole crystals are randomly oriented and may be coarse to very coarse grained. The amphibole may occur as disseminated crystals, in small aggregates of several crystals ("random" in Table 1), or in larger

TABLE 1. SUMMARY OF PETROGRAPHIC TYPES OF AMPHIBOLE, MACLELLAN GOLD DEPOSIT, MANITOBA

Type	Designation	Typical features	Fig.
Host-rock disseminated	metamorphic	Optically homogeneous, fine- to medium-grained, subidioblastic to idioblastic crystals with a preferred orientation	–
	random	Optically homogeneous, coarse-grained, single porphyroblasts or aggregates	2b
	zoned	Optically zoned, subidioblastic to idioblastic porphyroblasts	2c, 3b
Relict	relict	Isolated dark green crystals in massive alteration amphibole	3b, 3c
Patchy	patchy	Small aggregates of randomly oriented, typically poikiloblastic crystals	2a
Hydrothermal	vein	Aggregates of acicular crystals within quartz veins	4b
	alteration	Massive zones of fibrous to prismatic crystals; may or may not be vein-related	3b
	vug	Coarse, subidioblastic to idioblastic prismatic crystals interstitial to idioblastic crystals of quartz	4c
	vug-related	Coarse, poikiloblastic crystals surrounding chlorite–carbonate in vug	–

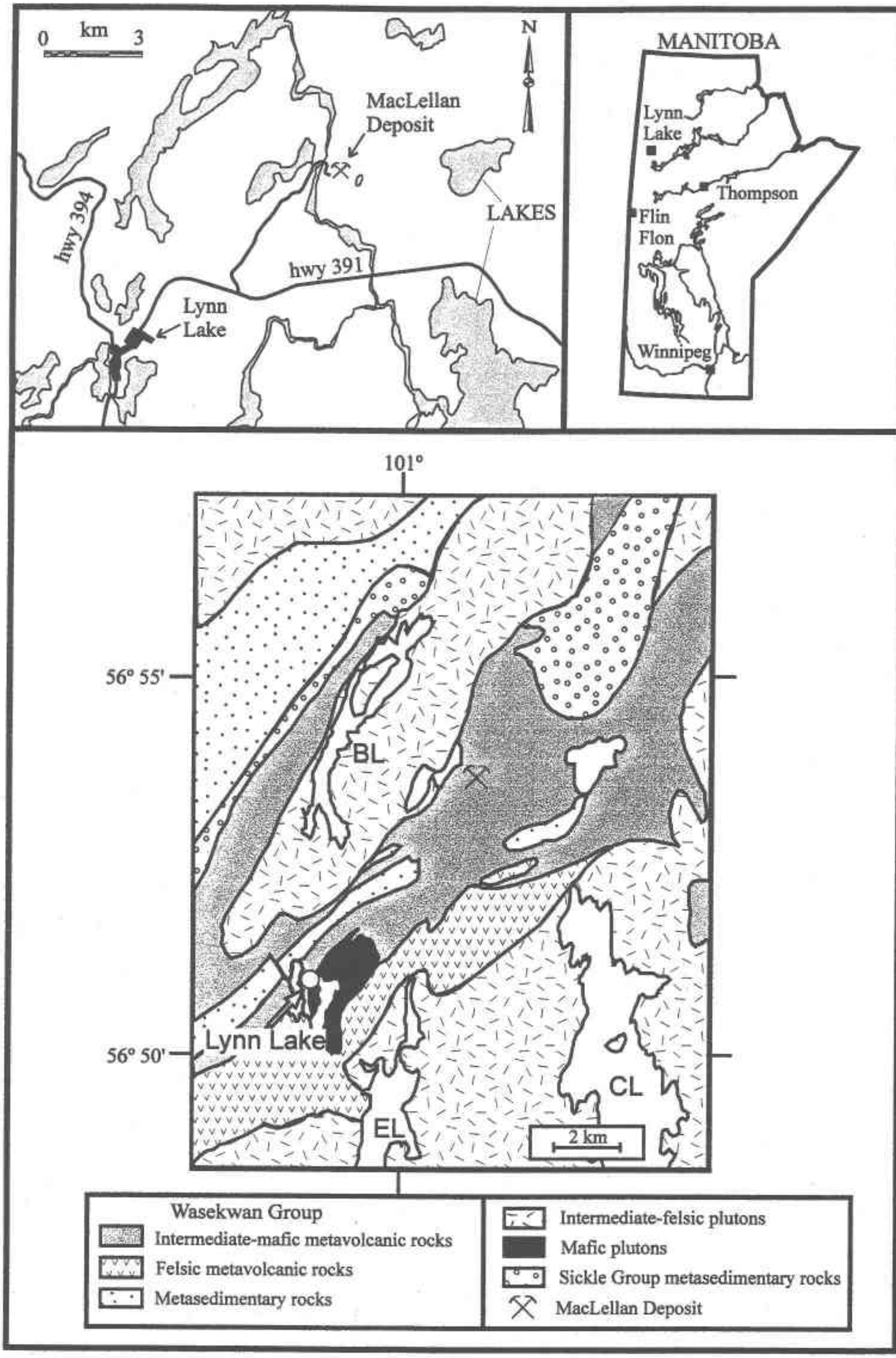

FIG. 1. Location of the MacLellan deposit, northern Manitoba. The local geology is based on maps GP80–1–1 and GP80–1–2, Manitoba Department of Energy and Mines (Gilbert *et al.* 1980). Symbols: BL: Burge Lake, EL: Eldon Lake, CL: Cockeram Lake.

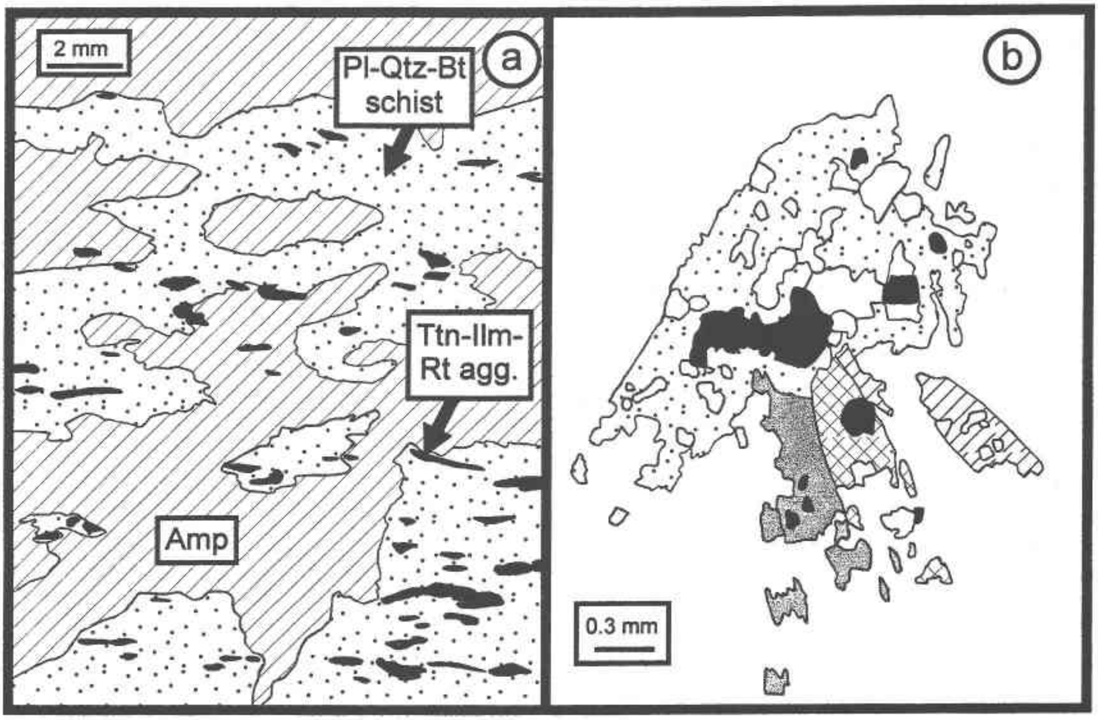

FIG. 2. (a) Patchy amphibole overprinting the fabric and replacing plagioclase – quartz – biotite schist; the titanite – ilmenite – rutile aggregates indicate the foliation. (b) Several coarse-grained, homogeneous poikiloblastic porphyroblasts (random grains of amphibole) have overprinted a plagioclase – biotite – quartz schist; inclusions are sphalerite and pyrite (black) and quartz and carbonate (white). Each pattern represents an individual crystal of amphibole. Symbols: Qtz: quartz, Bt: biotite, Pl: plagioclase, Ttn: titanite, Ilm: ilmenite, and Rt: rutile.

aggregates or patches of crystals (typically <1 cm across; "patchy" in Table 1; Fig. 2a). In a few samples, some grains of amphibole are conformable with the penetrative foliation and others cut across it, making textural discrimination difficult. In these cases, we have classified the amphibole as random on the basis of the cross-cutting varieties.

The randomly oriented crystals of amphibole vary considerably in texture, in part as a function of the matrix mineralogy. In quartz-rich lithologies, they are generally poikiloblastic, with inclusions of one or more of the following minerals: quartz, plagioclase, biotite, ilmenite, carbonate or, rarely, rutile (Fig. 2b), whereas in quartz-poor, biotite- or chlorite-rich lithologies, they are typically non-poikiloblastic. The randomly oriented amphibole crystals vary from idioblastic to xenoblastic, and include prismatic and acicular forms. In some samples, pale green prismatic and acicular varieties form radial aggregates. Typically, idioblastic crystals in biotite- and chlorite-rich units are zoned ("zoned" in Table 1). Zoned crystals generally comprise a dark green core and a light green to colorless rim (Fig. 3a). The cores are xenoblastic or mimic the idioblastic shape of the outer zone (Fig. 3a). Typically, only two zones are visible, but in some crystals, oscillatory zoning is developed toward the margin (Fig. 3a). Samples in which zoned crystals were observed also contain either coarse-grained, patchy aggregates of amphibole or pervasive alteration to massive amphibole (Fig. 3b). The amphibole in the aggregates is optically identical to that in the outer zone of the zoned porphyroblasts.

MINERALIZATION

The schists contain six mineralogically and texturally distinct types of veins and alteration: 1) quartz – biotite – sulfide (QBS) veins with biotite-rich alteration haloes, 2) quartz – arsenopyrite veins, 3) quartz – amphibole veins and patches with amphibole-rich alteration haloes, 4) vein and disseminated sulfides, 5) carbonate ± quartz veins and carbonate alteration, and 6) quartz ± sulfide veins (Samson & Gagnon 1995). In addition, rare sulfides of sedimentary origin are present in samples from the Nisku spoil heaps (Samson & Gagnon 1995). The QBS and quartz – arsenopyrite veins are the primary hosts to the gold mineralization, al-

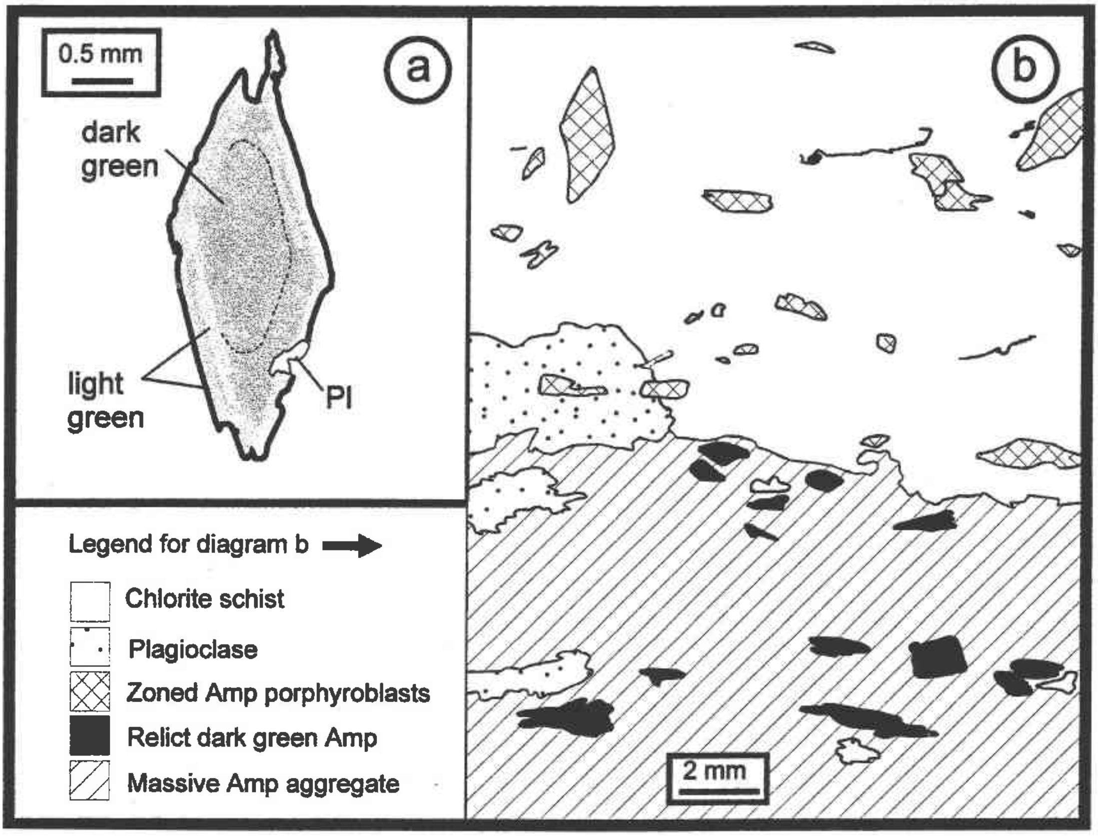

FIG. 3. (a) Porphyroblast of zoned amphibole in chlorite schist; dotted line marks a subtle change in color of core. (b) The top half of this diagram shows randomly oriented idioblastic zoned porphyroblasts in a chlorite schist. The lower half shows light-green massive alteration-related amphibole with darker green relict amphibole. The large crystal in the upper left is the zoned example shown in Figure 3a.

though elevated concentrations of gold also are associated with both the quartz – amphibole and quartz ± sulfide veins (Samson & Gagnon 1995). In the quartz–amphibole veins, the gold is probably related to the later sulfide veins and disseminated sulfides that overprint this stage. Textural studies (Samson & Gagnon 1995) indicate that the QBS veins predate metamorphism and the main event of deformation that produced the penetrative fabric; the quartz – arsenopyrite veins are broadly synmetamorphic, and the others are postmetamorphic. The quartz ± sulfide veins are related to late-stage brittle faults. Biotite and amphibole are by far the most abundant alteration-induced minerals in the deposit and are only associated with the QBS and quartz – amphibole veins. The other types of veins have little or no associated alteration and shall not be discussed further.

QBS veins are generally narrow (0.1 to 5 cm), highly deformed (folded and boudinaged) and consist of quartz ± biotite ± gahnite and sulfide minerals (pyrite, pyrrhotite, sphalerite, galena, arsenopyrite, chalcopyrite and boulangerite). These veins are almost exclusively hosted by the BP schists. In some samples, the veins have a narrow (typically <1 cm) halo in which the biotite content is higher than in the surrounding schist (Fig. 4a). In some cases, the halo is 100% biotite. These are particularly obvious in biotite-poor lithologies and less so in biotite-rich hosts. Where a halo is developed, the orange-brown biotite may be either randomly oriented or concordant with the penetrative foliation of the surrounding schist. The light brown biotite from the host rock will be referred to as "metamorphic", that in the haloes of the QBS veins as "vein-related", and biotite actually in the vein as "vein-hosted".

Quartz – amphibole veins are generally wider (≤10 cm) than QBS veins and continuous over greater distances (≤5 m). These veins are commonly boudinaged and disconformable to the foliation. The associated amphibole-rich halo overprints the foliation. The

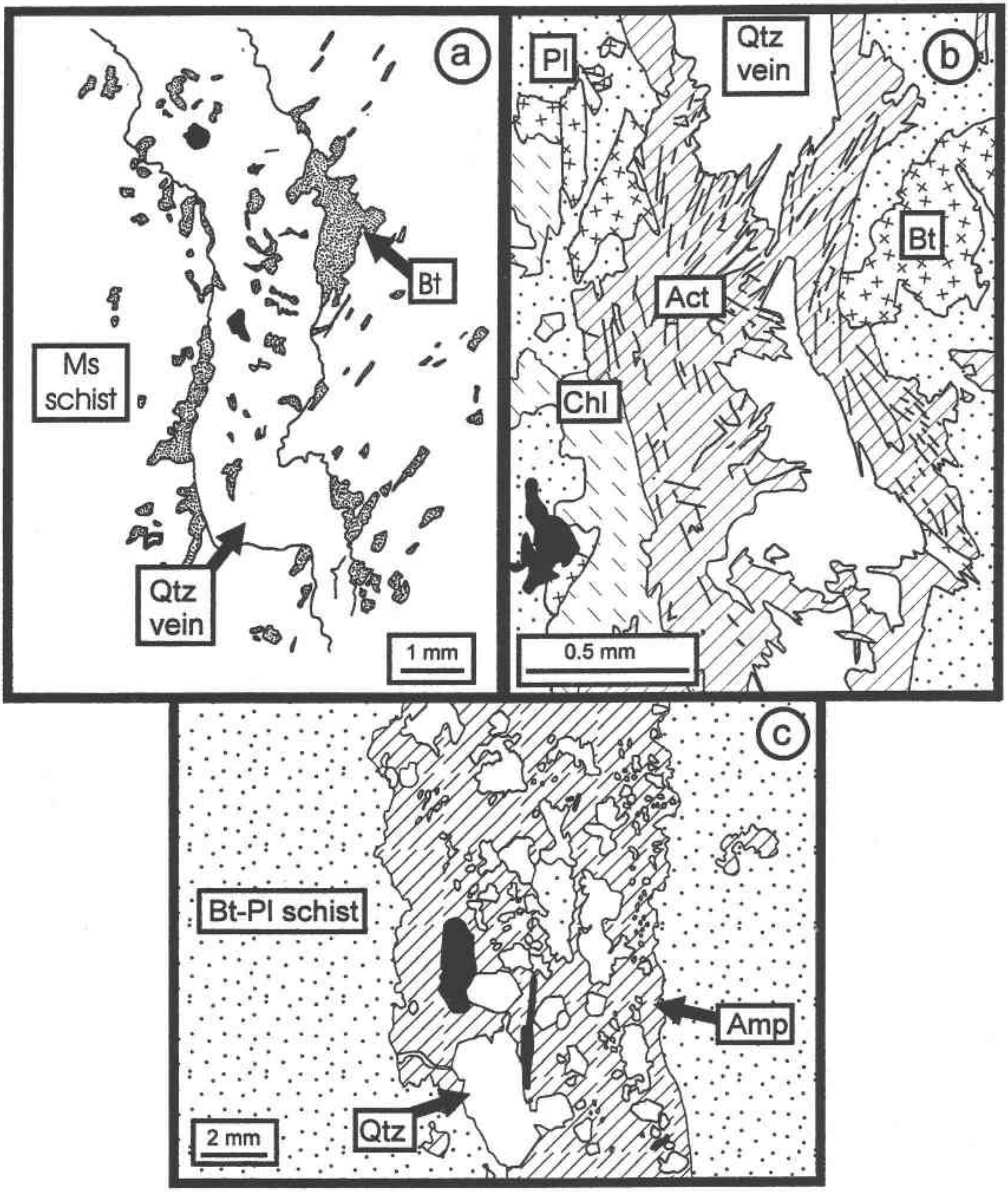

FIG. 4. (a) QBS vein with biotite halo; note that the vein is folded and that the penetrative foliation runs NE–SW across the figure. (b) Vein actinolite along the margin of a quartz vein. (c) Vug amphibole in biotite – plagioclase schist; note that the amphibole in this case encloses quartz crystals, some of which are idioblastic. Symbols: Ms: muscovite, Act: actinolite, and Chl: chlorite.

quartz–amphibole veins are therefore interpreted as a post-peak metamorphic, late-kinematic feature (Samson & Gagnon 1995). This stage also is manifested as discontinuous pods and patches of quartz in irregular zones of massive amphibole alteration and as zones of massive amphibole, both independent of obvious veins (referred to as "alteration" amphibole, Table 1). The veins are generally dominated by quartz with lesser amounts of amphibole, sulfide (pyrrhotite and sphalerite) and carbonate, and rare biotite and chlorite. In most veins, the sulfide and carbonate postdate the other minerals and represent a temporally distinct event. The amphibole within veins and enclosed in quartz is generally a fibrous, pale green to colorless variety ("vein" in Table 1; Fig. 4b). Alteration amphibole is typical of the host rocks to these veins and shows considerable variation in its textural and optical characteristics. Some veins have an amphibole-rich (80–100% by vol.) alteration halo that extend up to about 10 cm away from the vein margins. The amphibole in such haloes is generally pale green to colorless and is xenoblastic, prismatic, acicular or feathery. Such aggregates of massive amphibole are typical of quartz-poor lithologies and are best developed in CH schists, but they also occur in BP schists. Some massive aggregates contain coarse-grained, interstitial plagioclase enclosing fine-grained, acicular crystals of amphibole. In quartz-rich lithologies, the alteration is less pervasive and consists of coarse, poikiloblastic crystals of the same type of amphibole. The coarse alteration-related amphibole replaces and overprints the margins of the quartz veins. In some samples, crystals of massive, pale green alteration-related amphibole contain crystals of dark green xenoblastic, relict amphibole ("relict" in Table 1; Fig. 3b).

The alteration-induced amphibole crystals have been observed to overprint and replace *all* of the lithologies and mineral assemblages seen in the deposit. Quartz commonly occurs as inclusions, but is invariably corroded and clearly replaced in most cases. Idioblastic ilmenite is consistently preserved within the amphibole grains and is generally coarser than in the protolith. Coarse titanite is present in some amphibole assemblages and seems to be in equilibrium with both amphibole and ilmenite.

Some samples also contain small patches or vugs comprising coarse-grained idioblastic quartz surrounded by either coarse, dark green, subidioblastic to idioblastic amphibole ("vug" in Table 1; Fig. 4c), with coarse idioblastic biotite, pyrrhotite, pyrite, chalcopyrite, ilmenite ± titanite or, in one case, coarse biotite, chlorite, carbonate, pyrite, and sphalerite. The chlorite-bearing vug does not contain amphibole, but does occur within a patch of poikiloblastic amphibole, and may represent the patchy amphibole described above ("vug-related" in Table 1). These patches and vugs are distinguished from the veins and alteration described above by the fact that the quartz is commonly subidioblastic to idioblastic, the amphibole is interstitial to the quartz (rather than replacing it), they contain coarse, idioblastic biotite ("vug-related" in text that follows), and the sulfides and carbonate (in the case of the chlorite-bearing vug) occur interstitially to the silicates. These textures all suggest open-space deposition, possibly later than the other amphibole-bearing assemblages.

Mineral Composition

Samples were selected to represent all of the optical and textural variants of the amphibole and biotite. A total of 100 amphibole, 65 biotite and 15 chlorite analyses were made on a Cameca MBX electron microprobe at the University of Michigan, operated at a beam current of 20 nA at 15 kV. Reference standards included a range of natural oxide and silicate minerals; ZAF procedures provided by Cameca (Pouchou & Pichoir 1984) were used to correct compositions.

This paper focuses on the chemical composition of amphibole, biotite and chlorite produced during a complex history of deformation, metamorphism and metasomatism. Each of these minerals can contain a significant amount of Fe^{3+}, estimates of which are not available from the electron-microprobe data. Wet-chemical determinations of Fe_2O_3 are not useful in this study because of the small-scale variability of the minerals in question. Estimates of Fe^{3+}# values, where $Fe^{3+}\# = Fe^{3+}/(Fe^{3+} + Fe^{2+})$, based on the stoichiometry of phyllosilicates are generally unsatisfactory (*cf.* Dymek 1983, Guidotti 1984, Guidotti & Dyar 1991). Stoichiometry-derived estimates of Fe^{3+}# values in amphibole are, however, commonly made. Cosca *et al.* (1991) found that for calcic amphibole, a normalization based on 13 cations, exclusive of Ca, Na and K, gives reasonable estimates of ferric iron. The present International Mineralogical Association guidelines for amphibole classification recommend a procedure that averages normalizations, giving minimum and maximum Fe^{3+} estimates (Schumacher 1997), a technique very similar to that proposed by Spear & Kimball (1984). It remains, however, that estimation of the Fe^{3+} content of amphibole by stoichiometry is unsatisfactory; the scatter diagram comparing measured and calculated Fe^{3+} values given by Hawthorne (1983) is illustrative.

The principal control on the Fe^{3+}# values in the ferromagnesian minerals pertinent to this study, calcic amphibole, biotite and chlorite, is the oxidation potential, represented by the $f(O_2)$, during mineral formation (Spear 1981, Clowe *et al.* 1988, Guidotti & Dyar 1991, Dyar *et al.* 1992, Rebbert *et al.* 1995). Further, reasonable estimates of $f(O_2)$ can be made by considering the oxide and sulfide minerals in equilibrium with the silicate assemblage (Eugster & Skippen 1967, Holdaway *et al.* 1988, Williams & Grambling 1990).

In the rocks of the MacLellan deposit, amphibole, chlorite and biotite in unmineralized and unaltered host-rocks are typically associated with ilmenite (± rutile). Magnetite is locally observed in these rocks, but hematite is not found. Biotite and amphibole were therefore typically produced during metamorphism with ilmenite as the stable iron oxide phase. Amphibole and chlorite also were deposited by the fluids responsible for amphibole alteration in the presence of ilmenite ± titanite. Sulfide mineralization occurred during the history of the

TABLE 2. SUMMARY OF MINERAL ASSEMBLAGES IN SAMPLES FROM THE MacLELLAN DEPOSIT, MANITOBA

Sample	Main assemblage		Mgt	Rt	Ilm	Ttn	Sul
ALS–3	Pl–Qtz–Chl–Amp	*amphibole*		X			x
ALS–5	Chl–Bt–Pl–Amp	*amphibole*			X		X
		biotite		x	X		
N7	Qtz–Pl–Amp–Bt–St	*amphibole*	x		X		X
		biotite	x		X		
RSL–1	Bt–Qtz–Amp	*amphibole*			X		x
		biotite			X		x
ACD–8	Bt–Chl–Qtz–Amp	*amphibole*	X		x		
		biotite	X		x		
ACD–10	Chl–Bt–Amp–Qtz	*amphibole*		x	X		X
		biotite		x	X		X
ACD–22	Bt–Qtz–Amp–Pl	*amphibole*			X	x	X
		biotite			X	x	x
ACD–40a	Qtz–Bt	*biotite*		x	x	x	X
ACD–41a	Qtz–Bt	*biotite*		x	x		
ACD–43a	Qtz–Bt	*biotite*		x			X
ACD–43b	Qtz–Bt–Pl	*biotite*		x	X	x	X
ACD–45	Qtz–Bt–Chl	*biotite*		x			X
ACD–48	Qtz–Bt–Pl	*biotite*			X	x	X
ACD–53	Chl–Qtz–Bt–Amp	*amphibole*		x	X		X
		biotite		x	X		
ACD–60	Pl–Qtz–Bt–Amp	*amphibole*		x	x		x
ACD–64	Amp–Pl–Chl	*amphibole*			X		X
ACD–65	Qtz–Pl–Bt–Amp	*amphibole*	x		x		x
ACD–78	Bt–Amp–Pl	*amphibole*			X		X
		biotite			X		x
ACD–82	Qtz–Pl–Bt–Amp	*amphibole*			x	x	X
		biotite			x	x	X
ACD–84	Qtz–Pl–Bt–Amp	*amphibole*	x	x	x		x
		biotite	x	x	x		X
ACD–123	Chl–Amp	*amphibole*			X		
ACD–123	Pl–Bt–Amp	*amphibole*			X		X
ACD–155	Amp	*amphibole*			x	x	X
ACD–186	Qtz–Pl–Bt–Amp	*amphibole*			X	x	X
		biotite			X		
ACD–219	Qtz–Pl–Bt	*biotite*					X
ACD–222	Qtz–Pl–Bt–St	*biotite*		x			X
ACD–224	Qtz–Bt–Amp	*amphibole*		x			X
ACD–228	Bt–Amp–Pl–Qtz	*amphibole*			X		X
		biotite			X		

Mineral abbreviations are those of Kretz (1983), with the addition of Amp: amphibole, Mgt: magnetite, Ttn: titanite, Sul: sulfides (principally pyrite, pyrrhotite, arsenopyrite). X: abundant, x: sparse.

TABLE 3. REPRESENTATIVE COMPOSITIONS OF AMPHIBOLES FROM THE MacLELLAN DEPOSIT

Sample	ALS –5	ACD –53	ACD –186	ACD –64	ACD –64	ACD –60	ACD –2	ACD –65	ACD –84
Analysis	A–27	C–34	B–30	E–24	E–25	C–19	F–21	E–47	B–25
Description	relict	dissem. rand.	dissem. orient.	zoned core	zoned rim	massive	patchy	vein	vug
SiO_2 wt.%	44.97	51.61	51.21	44.98	46.57	51.68	49.85	50.88	45.45
TiO_2	0.25	0.31	0.06	0.31	0.41	0.29	0.37	0.30	0.34
Al_2O_3	12.72	6.40	6.63	13.22	11.04	5.05	7.45	6.13	11.79
Fe_2O_3**	3.18	2.31	2.60	3.65	2.05	1.70	1.94	1.82	4.69
Cr_2O_3	0.86	0.00	0.00	0.00	0.00	0.00	0.00	0.00	0.00
FeO**	9.87	7.15	8.06	11.33	10.45	8.65	9.88	9.29	9.85
MnO	0.89	0.41	0.63	0.43	0.51	0.54	0.25	0.71	1.02
MgO	12.53	17.08	15.86	10.81	13.28	16.64	14.64	16.18	12.16
CaO	11.61	12.29	12.34	11.80	12.43	12.50	12.65	12.07	11.31
Na_2O	0.82	0.33	0.36	0.78	0.62	0.30	0.46	0.27	1.02
K_2O	0.08	0.07	0.12	0.23	0.20	0.04	0.16	0.07	0.19
F	0.00	0.00	0.01	0.00	0.04	0.06	0.09	0.00	0.00
Cl	0.01	0.00	0.01	0.00	0.01	0.01	0.02	0.01	0.01
O=F,Cl	0.00	0.00	0.01	0.00	0.02	0.03	0.04	0.00	0.00
Total	97.79	97.96	97.89	97.54	97.59	97.42	97.71	97.73	97.82
H_2O Calc.*	2.05	2.11	2.09	2.03	2.04	2.06	2.03	2.09	2.03
Corr. Total	99.84	100.08	99.98	99.57	99.63	99.48	99.75	99.82	99.86
Structural formulae based on 23 O									
Si *apfu*	6.579	7.324	7.325	6.630	6.780	7.410	7.184	7.306	6.690
$^{[4]}Al$	1.421	0.676	0.675	1.370	1.220	0.590	0.816	0.694	1.310
T site	8.000	8.000	8.000	8.000	8.000	8.000	8.000	8.000	8.000
$^{[6]}Al$	0.773	0.395	0.442	0.926	0.675	0.263	0.449	0.344	0.736
Fe^{3+}**	0.234	0.164	0.187	0.270	0.150	0.122	0.140	0.131	0.346
Fe^{2+}	1.134	0.794	0.983	1.394	1.248	1.027	1.226	1.029	1.212
Ti	0.028	0.033	0.006	0.034	0.045	0.031	0.040	0.032	0.038
Mg	2.733	3.614	3.382	2.375	2.882	3.557	3.145	3.464	2.668
Cr	0.099	0.000	0.000	0.000	0.000	0.000	0.000	0.000	0.000
C site	5.000	5.000	5.000	5.000	5.000	5.000	5.000	5.000	5.000
Mn	0.110	0.049	0.076	0.054	0.063	0.066	0.031	0.086	0.127
Fe^{2+}	0.190	0.137	0.075	0.137	0.099	0.071	0.035	0.153	0.173
Ca	1.820	1.869	1.891	1.864	1.939	1.920	1.953	1.857	1.784
B site	2.121	2.055	2.042	2.054	2.101	2.057	2.019	2.096	2.084
Na	0.233	0.091	0.100	0.223	0.175	0.083	0.129	0.075	0.291
K	0.015	0.013	0.022	0.043	0.037	0.007	0.029	0.013	0.036
A site	0.247	0.103	0.122	0.266	0.212	0.091	0.158	0.088	0.327
OH*	1.998	2.000	1.993	2.000	1.979	1.970	1.954	1.998	1.998
F	0.000	0.000	0.005	0.000	0.018	0.027	0.041	0.000	0.000
Cl	0.002	0.000	0.002	0.000	0.002	0.002	0.005	0.002	0.002
Mg#	0.674	0.795	0.762	0.608	0.682	0.764	0.714	0.746	0.658

* H_2O by back-calculation of structural formulae assuming 2 (OH, F, Cl).
** Fe^{3+} and Fe^{2+} estimated by assuming a value of $Fe^{3+}/(Fe^{3+} + Fe^{2+})$ derived from the mineral assemblage (see text). Abbreviations: rand: random, orient.: oriented.

deposit: with QBS-stage veining, during the peak of metamorphism (quartz – arsenopyrite veins) and after the amphibole alteration. A summary of the dominant and accessory mineralogy for the MacLellan rocks is given in Table 2.

The metamorphic assemblages that include ilmenite or rutile as the only oxide minerals probably formed at an $f(O_2)$ close to the QFM buffer (Holdaway *et al.* 1988, Williams & Grambling 1990). Those metamorphic rocks containing magnetite were formed under conditions more oxidizing than QFM but below HM; conditions approximating the NNO buffer are assumed for the magnetite-bearing rocks. Ilmenite was the only iron oxide stable during the amphibole-stage alteration; these assemblages are considered to have been produced under QFM conditions.

We assume that amphibole formed under NNO and QFM buffers has Fe^{3+}# values of 0.30 and 0.20, respectively (Clowe *et al.* 1988). Biotite produced at the QFM buffer has an Fe^{3+}# value of 0.12 (Guidotti & Dyar 1991, Holdaway *et al.* 1997). Biotite occurring with magnetite and ilmenite is assumed to be produced at conditions close to the NNO buffer and to have a Fe^{3+}# of 0.20 (Dyar 1990, Guidotti & Dyar 1991). Dyar (1990) and Guidotti & Dyar (1991) stated that 8% of the total Fe in biotite occurs as $^{[4]}Fe^{3+}$; later studies by Rancourt *et al.* (1992), however, show that very little Fe^{3+} is in the tetrahedral site. We therefore assume that all Fe^{3+} is in the octahedral site.

TABLE 4. REPRESENTATIVE COMPOSITIONS OF BIOTITE FROM THE MACLELLAN DEPOSIT

	host-rock disseminated metamorphic			QBS stage vein-hosted		QBS stage vein-related		amphibole stage	
Sample	ACD –10	ACD –22	ACD –53	ACD –40A	ACD –43B	ACD –48	ACD –40A	ACD –84	ACD –82
Analysis	F-12	F-23	C-30	F-31	E-51	E-40	F-30	B-14	A-15
SiO_2 wt.%	37.66	37.78	38.29	37.58	37.34	37.36	37.62	38.65	36.09
TiO_2	1.69	1.90	1.44	2.43	2.38	2.84	2.31	1.36	1.91
Al_2O_3	16.75	17.16	17.23	16.78	16.80	16.75	16.79	16.73	16.93
Fe_2O_3**	3.95	1.81	1.57	1.91	1.88	2.24	2.07	3.43	2.11
Cr_2O_3	0.59	0.05	0.00	0.02	0.04	0.01	0.08	0.00	0.11
FeO**	14.22	12.39	10.73	13.12	12.92	15.33	14.21	12.34	14.45
MnO	0.04	0.07	0.09	0.41	0.45	0.38	0.53	0.21	0.23
MgO	12.15	14.92	17.19	13.46	14.23	11.88	12.92	14.99	15.30
CaO	0.04	0.03	0.09	0.00	0.00	0.01	0.03	0.02	0.08
Na_2O	0.19	0.15	0.22	0.09	0.08	0.14	0.14	0.16	0.17
K_2O	9.07	9.27	8.60	9.83	9.26	9.34	9.45	8.33	8.27
F	0.14	0.10	0.24	0.10	0.21	0.16	0.18	0.17	0.55
Cl	0.02	0.03	0.02	0.02	0.01	0.03	0.04	0.00	0.00
O=F,Cl	0.06	0.05	0.11	0.05	0.09	0.07	0.08	0.07	0.23
Total	96.45	95.61	95.60	95.71	95.52	96.39	96.29	96.31	95.97
H_2O Calc.*	3.95	4.01	4.01	3.98	3.95	3.95	3.95	4.02	3.80
Corr. Total	100.41	99.63	99.62	99.69	99.46	100.34	100.24	100.33	99.77
Structural formulae based on 22 O									
Si *apfu*	5.610	5.567	5.555	5.585	5.532	5.561	5.574	5.655	5.327
$^{[4]}$Al	2.390	2.433	2.445	2.415	2.468	2.439	2.426	2.345	2.673
T site	8.000	8.000	8.000	8.000	8.000	8.000	8.000	8.000	8.000
$^{[6]}$Al	0.551	0.547	0.501	0.524	0.465	0.499	0.506	0.539	0.272
Ti	0.189	0.211	0.157	0.272	0.265	0.318	0.257	0.150	0.212
Fe^{3+}	0.443	0.200	0.171	0.214	0.210	0.250	0.231	0.377	0.234
Cr	0.069	0.006	0.000	0.002	0.005	0.001	0.009	0.000	0.013
Fe^{2+}	1.772	1.527	1.302	1.631	1.601	1.908	1.761	1.509	1.784
Mn	0.005	0.009	0.011	0.052	0.057	0.048	0.067	0.026	0.029
Mg	2.698	3.278	3.718	2.982	3.143	2.636	2.854	3.269	3.366
M site	5.729	5.778	5.859	5.676	5.746	5.660	5.686	5.871	5.910
Ca	0.006	0.005	0.014	0.000	0.000	0.002	0.005	0.003	0.013
Na	0.055	0.043	0.062	0.026	0.023	0.040	0.040	0.045	0.049
K	1.724	1.743	1.592	1.864	1.750	1.773	1.786	1.555	1.557
I site	1.785	1.790	1.667	1.890	1.773	1.815	1.831	1.603	1.618
OH Calc.*	3.929	3.946	3.885	3.948	3.899	3.917	3.906	3.921	3.743
F	0.066	0.047	0.110	0.047	0.098	0.075	0.084	0.079	0.257
Cl	0.005	0.007	0.005	0.005	0.003	0.008	0.010	0.000	0.000
Mg/(Mg+Fe^{2+})	0.604	0.682	0.741	0.646	0.662	0.580	0.618	0.684	0.654

* H_2O by back-calculation of structural formulae assuming 4 (OH, F, Cl). ** The proportion of Fe^{3+} and Fe^{2+} was estimated by assuming a value of $Fe^{3+}/(Fe^{3+} + Fe^{2+})$ derived from the mineral assemblage (see text).

TABLE 5. REPRESENTATIVE COMPOSITIONS OF CHLORITE FROM THE MACLELLAN DEPOSIT

Sample	ACD –123a	ACD –228	ACD –60	ACD –8	ACD –84	ACD –84	ALS –5
Analysis	F-03	C-33	C-06	A-20	B-11	B-12	A-31
Type	HD	HD	HD	HD	vug	vug	HD
SiO_2 wt.%	26.56	26.45	26.14	25.87	26.20	26.78	26.05
TiO_2	0.12	0.06	0.06	0.10	0.07	0.10	0.06
Al_2O_3	22.94	22.59	22.41	22.80	21.63	21.24	22.65
Fe_2O_3**	1.54	1.52	1.64	2.68	1.97	1.91	1.44
Cr_2O_3	0.05	0.00	0.00	0.00	0.00	0.00	0.18
FeO**	12.44	12.35	13.27	21.69	15.95	15.44	11.64
MnO	0.23	0.17	0.23	0.22	0.38	0.40	0.39
MgO	23.19	24.41	23.43	14.80	21.12	21.97	25.23
CaO	0.03	0.02	0.00	0.03	0.02	0.01	0.05
Na_2O	0.00	0.02	0.01	0.02	0.02	0.02	0.02
K_2O	0.00	0.00	0.02	0.01	0.00	0.01	0.00
F	0.03	0.00	0.09	0.17	0.05	0.00	0.00
Cl	0.00	0.01	0.00	0.03	0.00	0.00	0.01
O = F, Cl	0.01	0.00	0.04	0.08	0.02	0.00	0.00
Total	87.10	87.61	87.25	88.31	87.39	87.87	87.72
H_2O calc.*	12.01	12.08	11.92	11.47	11.75	11.88	12.10
Corr. Total	99.11	99.69	99.17	99.78	99.14	99.75	99.82
Structural formulae based on 28 O							
Si *apfu*	5.301	5.253	5.243	5.368	5.336	5.405	5.162
$^{[4]}$Al	2.699	2.747	2.757	2.632	2.664	2.595	2.838
T site	8.000	8.000	8.000	8.000	8.000	8.000	8.000
$^{[6]}$Al	2.696	2.541	2.542	2.944	2.526	2.457	2.452
Ti	0.018	0.010	0.009	0.016	0.011	0.015	0.009
Fe^{3+}	0.231	0.228	0.247	0.418	0.302	0.290	0.214
Cr	0.007	0.000	0.000	0.000	0.000	0.000	0.028
Fe^{2+}	2.075	2.051	2.226	3.764	2.715	2.606	1.929
Mn	0.039	0.029	0.039	0.038	0.066	0.068	0.065
Mg	6.898	7.226	7.004	4.577	6.411	6.610	7.455
Ca	0.007	0.004	0.000	0.006	0.005	0.003	0.011
Na	0.000	0.008	0.004	0.009	0.009	0.009	0.009
K	0.000	0.000	0.005	0.002	0.000	0.001	0.000
M site	11.971	12.095	12.076	11.774	12.045	12.059	12.172
OH*	15.983	15.996	15.945	15.882	15.966	16.000	15.996
F	0.017	0.000	0.055	0.110	0.034	0.000	0.000
Cl	0.000	0.004	0.000	0.004	0.000	0.000	0.004
Mg/(Mg+Fe^{2+})	0.769	0.779	0.759	0.549	0.702	0.717	0.794

* H_2O by back-calculation of structural formulae assuming 16 (OH,F,Cl). ** The proportion of Fe^{3+} and Fe^{2+} was estimated by assuming Fe^{3+} = 10% of total Fe (see text).

Nelson & Guggenheim (1993) showed that oxidation of Fe^{2+} to Fe^{3+} in chlorite is limited to the *M*4 "interlayer" position. Thus chlorite should be relatively insensitive to $f(O_2)$. Dyar *et al.* (1992) showed that chlorites from a wide variety of environments and oxide-mineral assemblages all have a small but significant Fe^{3+} content, which they estimate to be 10 ± 5% of the total Fe. This value is used in our calculation of chlorite formulae, with the proportion of Fe_2O_3 and FeO being back-calculated from stoichiometry.

Amphibole compositions were first assessed by normalization to 23 atoms of oxygen assuming all Fe as Fe^{2+}. Those compositions that did not generate a reasonable formula (three out of 100 datasets) were rejected. Amphibole formulae were then calculated assuming 23 O, 2 (OH, F, Cl) and a Fe^{3+}# value appropriate to the mineral assemblage. Amphibole compositions representative of each textural type are given in Table 3.

The composition of biotite in each petrographic assemblage of the MacLellan deposit is given in Table 4. Structural formulae based on 22 atoms of oxygen were calculated using the procedure of Deer *et al.* (1992) by assuming a value of Fe^{3+}# that reflects the assemblage of oxide minerals. The proportion of H_2O was back-calculated assuming 4 (OH, F, Cl).

Representative chlorite compositions are given in Table 5. Structural formulae were calculated assuming

28 O, 16 (OH, F, Cl) and a value of Fe^{3+}# of 0.10 (Dyar *et al.* 1992).

Amphibole

Amphibole compositions representative of each textural type (Table 2) reveal significant variations. If all textural types are considered together, most of the MacLellan material falls within the compositional ranges of typical metamorphic amphiboles, as documented by Robinson *et al.* (1982). For a given crystallographic site, however, the MacLellan suite typically covers a significant part of the compositional range exhibited by metamorphic amphiboles. This is particularly true for $^{[4]}Al$, $^{[6]}Al$, Fe^{2+}, Mg and ^{A}Na. The Mg# [= Mg/(Mg + Fe)] varies from 0.39 to 0.90, and ^{A}Na ranges from 0.01 to 0.37 atoms per formula unit (*apfu*). ^{B}Ca occupancy in the MacLellan amphiboles, with values of 1.63 to 1.97 *apfu*, falls within the high-Ca group of metamorphic amphiboles (Robinson *et al.* 1982). All the MacLellan amphiboles have $^{B}(Ca + Na)$ in excess of 1.70 and ^{B}Na less than 0.38 *apfu*. Thus, they are all calcic amphiboles according to the IMA classification (Leake *et al.* 1997). Although the MacLellan amphiboles exhibit a wide range of $^{[6]}Al/Fe^{3+}$ values (0.02–4.21), ^{C}Ti values are all less than 0.08 *apfu*, and $^{A}(Na + K)$ values are less than 0.42 *apfu*. The wide range in composition of the calcic amphiboles is reflected in their classification (Fig. 5). The species identified are ferrotschermakite, tschermakite, magnesiohornblende, and actinolite.

Relative to tremolite (*cf.* Robinson *et al.* 1982, Blundy & Holland 1990, Castro & Stephens 1992), the more important substitutions seem to be actinolitic ($^{C}Fe^{2+}Mg_{-1}$) (Fig. 5) and pargasitic ($^{A}Na^{[6]}Al^{[4]}Al_2 \square_{-1}Mg_{-1}Si_{-2}$) (Fig. 6), the latter being a combination

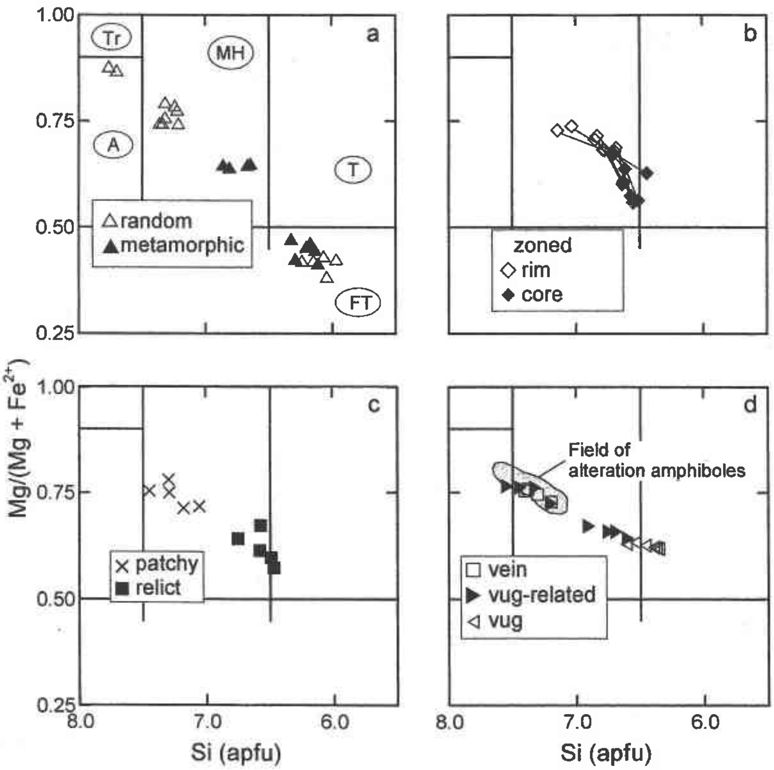

FIG. 5. Plots of Si (*apfu*) *versus* $Mg/(Mg + Fe^{2+})$ for amphiboles. (a) Metamorphic and random crystals; the former have a preferred orientation, and the latter overprint the penetrative fabric. (b) Zoned crystals, illustrating the chemical differences between cores and rims. Tie-lines connect cores and rims of the same crystal. (c) Patchy and relict crystals. (d) Compositions of probable hydrothermal amphibole, comprising alteration, vein, interstitial and vug varieties. Amphibole classification after Leake *et al.* (1997): Symbols: Tr: tremolite, A: actinolite, MH: magnesiohornblende, T: tschermakite, and FT: ferrotschermakite.

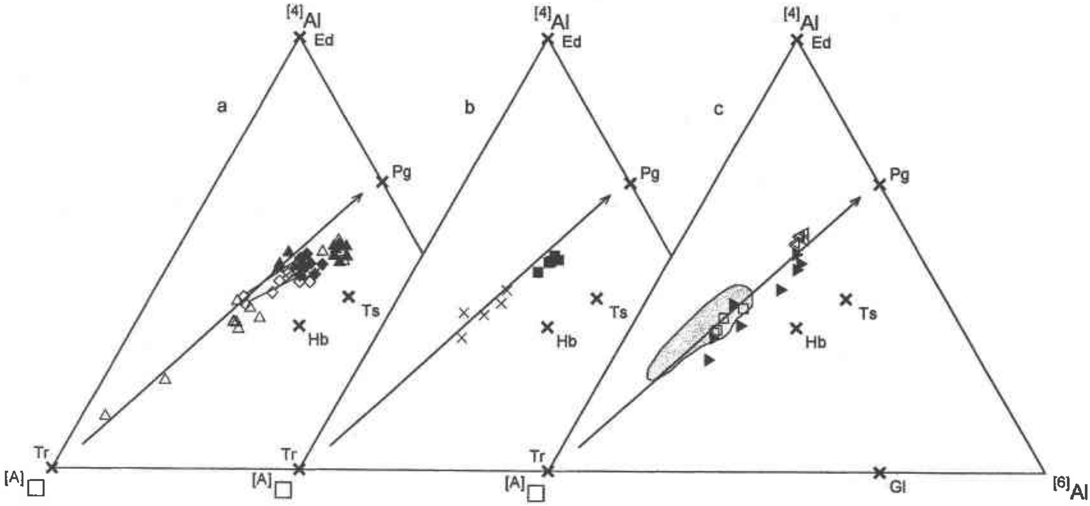

FIG. 6. Compositions of the various textural types of amphibole in terms of [4]Al, [6]Al and [A]□ illustrating the predominance of a pargasitic substitution (after Blundy & Holland 1990). Symbols are the same as in Figure 5. Ed: edenite, Pg: pargasite, Ts: tschermakite, Hb: magnesiohornblende or ferrohornblende, Tr: tremolite, and Gl: glaucophane. (a) Metamorphic, random and zoned crystals (*cf.* Figs. 5a, b); (b) patchy and relict crystals (*cf.* Fig. 5c), and (c) alteration, vein and vug crystals (*cf.* Fig. 5d).

of edenite and tschermakite substitutions, $^{A}Na^{[4]}Al\,\square_{-1}Si_{-1}$ and $^{[4]}Al^{[6]}AlMg_{-1}Si_{-1}$, respectively (Blundy & Holland 1990). Grains of relict amphibole, the cores of zoned crystals and the vug and vug-related amphiboles form a rather tight compositional group from tschermakite to aluminous magnesiohornblende (Figs. 5b, c, d, 6a, b, c). The rims of zoned crystals are more magnesian and less aluminous than the cores (Figs. 5b, 6a) and are similar in composition to grains of patchy amphibole (Figs. 5c, 6b) and to vein and alteration amphiboles (Figs. 5d, 6c). This latter group ranges in composition from aluminum-poor magnesiohornblende to actinolite. In the host rock, the grains of amphibole are classified petrographically as either metamorphic (oriented) or random. It is not possible to perfectly differentiate between these petrographic types by composition (Figs. 5a, 6a), although random crystals tend to be more magnesian, less aluminous and more enriched in the tremolite end-member than the metamorphic amphiboles. The compositions of random amphibole are similar to those for vein, alteration and patchy amphibole.

Biotite

The composition of biotite-series grains in each petrographic assemblage of the MacLellan deposit is presented in Table 4. Compositional data are also presented in the idealized annite – phlogopite – siderophyllite – eastonite plane (Fig. 7), which defines the biotite series (Rieder *et al.* 1998). The biotite-series minerals are, in general, Mg-rich, with a limited range in X_{Mg}, from 0.53

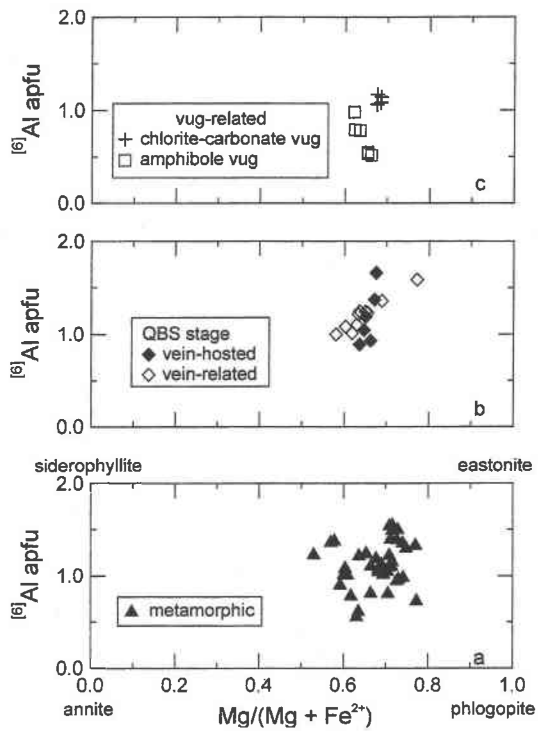

FIG. 7. Composition of biotite in terms of $Mg/(Mg + Fe^{2+})$ and [6]Al. (a) Metamorphic biotite, (b) QBS-stage biotite, and (c) vug-related biotite.

to 0.77, and can be defined as phlogopite–eastonite. A correlation of X_{Mg} with $^{[6]}Al$, indicating a Mg-Tschermak exchange, is weak for metamorphic host phlogopite–eastonite and well defined for QBS-stage biotite, which is dominated by eastonite. An Fe^{2+}-Tschermak exchange is indicated for phlogopite associated with amphibole vugs. Data for eastonite from the chlorite–carbonate vug, although distinct from the phlogopite associated with the amphibole vug, are too limited to define an exchange mechanism.

The concentrations of F and Cl in the MacLellan biotite are low (<0.26 *apfu* for F and <0.03 *apfu* for Cl; Table 4), even compared to biotite from other lode-gold deposits (*cf.* Taner *et al.* 1986, Kontak & Smith 1993). No correlations between Fe and Cl *versus* X_{Mg}, related to Fe avoidance, are evident (*cf.* Munoz & Swenson 1981).

The concentration of Ti in biotite correlates with the X_{Mg} of the biotite as well as the nature of the associated Ti phase (Fig. 8). One group of light to dark brown biotite grains with low Ti has no identified saturating phase or only minor rutile in the assemblage. The correlation of Ti with X_{Mg} in this group is probably controlled by the bulk composition of the rocks. Biotite grains, typically orange-brown, from assemblages containing rutile, ilmenite or ilmenite plus rutile, form a series with intermediate Ti content. A third group of bright orange-brown biotite grains with high Ti all have titanite in the assemblage along with ilmenite and rutile. Although the number of data is small, there is no obvious correlation between the color of biotite or its Ti content and the presence of magnetite.

Eastonite in and near QBS veins, along with a few occurrences in metamorphic rocks hosting QBS veins, dominate the high-Ti group (Fig. 8). This group has an average Ti content of 0.26 ± 0.03 *apfu* and an average X_{Mg} of 0.64 ± 0.02. Titanite, as a reaction rim around ilmenite or rutile (or both), is always part of the Ti-saturating assemblage in the high-Ti group. Metamorphic phlogopite–eastonite is associated with rutile ± ilmenite as the Ti-saturating phase(s). Magnetite, a probable Ti-bearing phase, locally occurs with ilmenite. Phlogopite–eastonite that formed with rutile as the dominant Ti-saturating phase has a lower Ti (0.16 ± 0.03 *apfu*) and is more magnesian (X_{Mg} = 0.70 ± 0.04) than that associated with ilmenite (Ti = 0.20 ± 0.03, X_{Mg} = 0.65 ± 0.06).

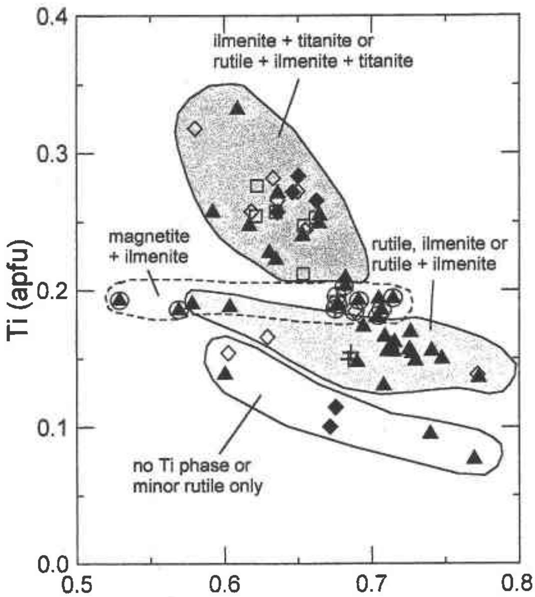

FIG. 8. Ti content of the various biotite subtypes as a function of $Mg/(Mg + Fe^{2+})$. The fields are defined on the basis of the coexisting oxide minerals. Symbols are the same as in Figure 7; where magnetite is present, the symbol is circled.

Chlorite

Except for host-rock metamorphic chlorite in a magnetite-rich assemblage (*e.g.*, chlorite B–11 in ACD–8, Table 5), the chlorite compositions are uniform compared to those for amphibole and biotite. On the basis of $O_{20}(OH)_{16}$, Si averages 5.26 ± 0.11 *apfu*, the balance of the eight tetrahedral positions being filled by Al. Values of $^{[4]}Al$ and $^{[6]}Al$ are approximately the same in all samples. Occupancy of the octahedral sites is close to 12 cations in all samples. Values of $Mg/(Mg + Fe^{2+})$ average 0.71 ± 0.10 and range from 0.51 to 0.79 for the whole dataset. If chlorite associated with abundant magnetite is removed from the dataset, however, the average $Mg/(Mg + Fe^{2+})$ increases to 0.76 ± 0.03, with a range of 0.70 to 0.79. The chlorite is considered metamorphic, except for two samples from the chlorite – carbonate vug, in which it has a hydrothermal origin.

Mineral pairs

The various mineral associations representative of metamorphosed host-rocks, QBS veins, and amphibole veins and alteration can be evaluated by examining the distribution of iron and magnesium among coexisting ferromagnesian minerals. The distribution coefficient K_D, *i.e.*, $(X_{Mg}^A/X_{Fe}^A)/(X_{Mg}^B/X_{Fe}^B)$, where A and B are coexisting phases, depends principally on temperature and pressure. It is also a function of the mineral assemblage and phase composition. In the analysis that follows, K_D is presented by simple Nernst distribution diagrams, where X_{Mg}^A is plotted against X_{Mg}^B (*cf.* Kretz 1959, 1978). In some cases, the mineral pairs described are in contact and are most likely cogenetic; for these, an equilibrium distribution is expected. However, in many cases, the two minerals are not in contact

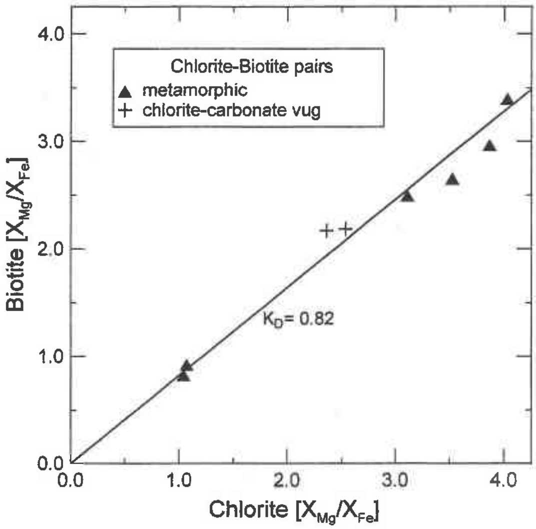

FIG. 9. X_{Mg}/X_{Fe} distribution in biotite–chlorite pairs. The equilibria represented by these pairs can be described by a single K_D.

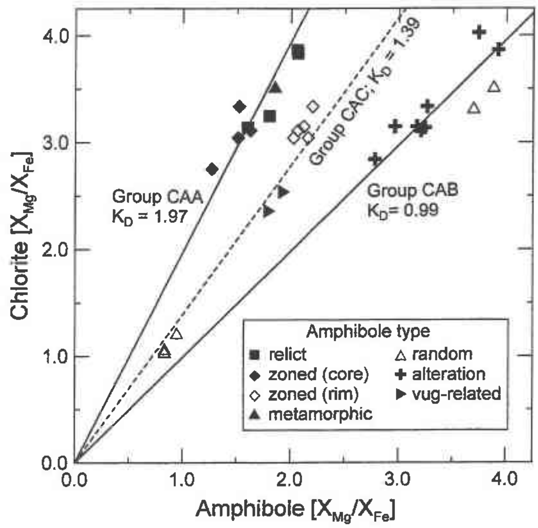

FIG. 10. X_{Mg}/X_{Fe} distribution in chlorite–amphibole pairs. The compositions of these chlorite–amphibole pairs indicate three different equilibria. In terms of amphibole type, Group CAA is defined by metamorphic crystals, the cores of zoned crystals, and relict crystals. Group CAB comprises vein and alteration amphibole, and some random porphyroblasts of amphibole. Group CAC is defined by the rims of zoned crystals, vug-related crystals of amphibole and random porphyroblasts of amphibole.

(although always in the same thin section), or one mineral may be overgrowing and replacing the other, as previously described. For such pairs, an equilibrium distribution can only be expected within the spatial limits of local equilibrium (*cf.* Blackburn 1968).

Relatively few chlorite – biotite pairs were analyzed, but are representative of both metamorphic assemblages and the chlorite – carbonate vug, and can be approximately described by a single K_D (Fig. 9, Table 6).

Chlorite – amphibole pairs define one of three equilibrium distributions (Fig. 10, Table 6). The first, Group CAA with K_D = 1.97, is defined by relict amphiboles, the cores of zoned amphibole crystals and the crystals of metamorphic amphibole. A second group (CAB; K_D = 0.99) consists mostly of alteration amphibole paired with metamorphic chlorite. Group CAB also includes two random amphibole grains. The chlorite in the third distribution (Group CAC; K_D = 1.39) comprises principally metamorphic chlorite along with the two cases of vug chlorite. The amphibole of this group is represented by rims of zoned crystals, two vug-related amphibole grains and three random amphibole grains. It is possible that the random amphibole grains of Group CAC actually belong to Group CAB.

Biotite – amphibole pairs define three groups (Fig. 11), which are very similar to those observed for chlorite–amphibole pairs (Fig. 10). Group BAA, with K_D = 1.41, contains metamorphic biotite with metamorphic and relict amphibole. Group BAB (K_D = 0.88) com-

TABLE 6. SUMMARY OF Fe–Mg DISTRIBUTIONS FOR COEXISTING CHLORITE–BIOTITE, CHLORITE–AMPHIBOLE AND BIOTITE–AMPHIBOLE PAIRS, MACLELLAN DEPOSIT

chlorite–biotite	Group	chlorite types	biotite types	no. of pairs	$K_D^{bt/chl} \pm \sigma$
	CBA	metamorphic, chlorite–carbonate vug	metamorphic, chlorite–carbonate vug	8	0.82 ± 0.06
chlorite–amphibole	Group	chlorite types	amphibole types	no. of pairs	$K_D^{chl/amp} \pm \sigma$
	CAA	metamorphic	relict, zoned (cores), metamorphic	9	1.97 ± 0.14
	CAB	metamorphic	alteration, random	10	0.99 ± 0.06
	CAC	metamorphic, chlorite–carbonate vug	random, zoned (rims), vug-related	10	1.39 ± 0.11
biotite–amphibole	Group	biotite types	amphibole types	no. of pairs	$K_D^{bt/amp} \pm \sigma$
	BAA	metamorphic	relict, metamorphic	8	1.41 ± 0.12
	BAB	metamorphic	random, alteration, patchy	8	0.88 ± 0.03
	BAC	chlorite–carbonate vug, amphibole vug	random, amphibole vug, vug-related	10	1.07 ± 0.07

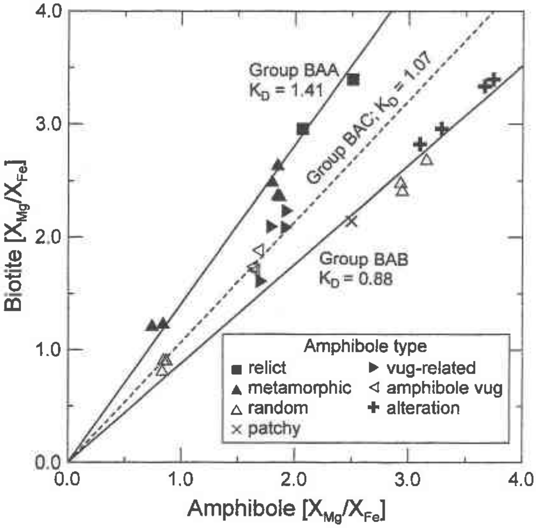

FIG. 11. X_{Mg}/X_{Fe} distribution in biotite and coexisting amphibole. As with chlorite–amphibole pairs, the K_D values of biotite–amphibole pairs indicate three different equilibria. Group BAA is defined by metamorphic biotite and metamorphic and relict amphibole. Group BAB comprises metamorphic biotite with alteration, random and patchy amphibole. Group BAC is defined by vug-related biotite and vug, vug-related and random amphibole.

prises metamorphic biotite with random, patchy and alteration amphiboles. Pairs of vug and vug-related amphibole grains and vug-related biotite as well as three random amphibole – metamorphic biotite pairs define a third group BAC (K_D = 1.07), intermediate to Groups BAA and BAB. The random amphibole – biotite pairs of Group BAC may belong to Group BAB.

Discussion

QBS stage

The petrographic evidence indicates that the formation of QBS veins predates metamorphism and deformation. Vein-related alteration is now manifested as a biotite-rich halo along many of the veins. Whether or not the premetamorphic alteration assemblage, at the expense of which the biotite crystallized, included biotite cannot be determined with certainty. However, the fact that biotite seems to be the only Fe–Mg silicate produced during metamorphism strongly suggests that the haloes represent recrystallization of an original biotite-bearing alteration. The alternative, that the biotite crystallized from an assemblage of minerals that may or may not have included biotite, would have resulted in a metamorphic assemblage with greater mineralogical variability than the one seen. Whether or not any of the biotite present in the schists away from the veins also reflects a potassic alteration event is impossible to assess from petrography alone, but is plausible, if not likely.

In terms of X_{Mg} and $^{[6]}$Al, biotite in and related to QBS veins has a more restricted compositional range than metamorphic biotite (Fig. 7). It is possible that the compositional range of metamorphic biotite reflects growth in rocks with a wide range of bulk compositions. Because the distribution of vein-related biotite was controlled by earlier hydrothermal effects, however, it is likely that the restricted range of vein and vein-related eastonite reflects fluid-buffered compositions. This claim is supported by the presence, in this population, of eastonite from haloes in rocks that otherwise contain very little biotite. Further, host-rock phlogopite–eastonite from near QBS veins defines an equally restricted range in X_{Mg}, but shows a somewhat higher variation in $^{[4]}$Al content. This variability may indicate that host-rock biotite in the vicinity of QBS veins has also been influenced by hydrothermal activity, especially with respect to Fe and Mg, and that some of the biotite in the BP schists represents a potassic alteration event. Finally, the QBS veins represent a major sulfide mineralization event. The ubiquitous presence of pyrite ± pyrrhotite would buffer $f(S_2)$ to low, but significant, values and limit Fe incorporation into ferromagnesian silicates in the veins and alteration haloes.

Concentrations of F and Cl in the eastonite of the QBS veins and vein haloes and in the later metamorphic phlogopite – eastonite are low. The X_F ranges from 0.012 to 0.033 in QBS vein-hosted eastonite and 0.004 to 0.026 in vein-related eastonite. Assuming the exchange relationship Mica$(OH)_2$ + 2HF = Mica$(F)_2$ + $2H_2O$ and a temperature of 400°C, the $f(HF)/f(H_2O)$ for QBS-stage deposition of eastonite is $10^{-5.2}$ to $10^{-4.8}$ (Zhu & Sverjensky 1991). A similar range of $f(HF)/f(H_2O)$ is found for the metamorphic phlogopite – eastonite.

The Ti content of biotite is controlled by temperature, Fe/Mg and $^{[4]}$Al in biotite and the nature of the Ti-saturating phase (Guidotti *et al.* 1977, Dymek 1983, Labotka 1983, Guidotti 1984). Weak relationships between Ti and X_{Mg} (Fig. 8) and Ti and $^{[4]}$Al are observed. Although kyanite is observed in some metamorphic assemblages, a phase with fixed Al is not found in most QBS-stage veins. Gahnite is present in some assemblages, but there is no correlation between $^{[4]}$Al in biotite and the presence of gahnite. Thus, the Al and Ti contents of the QBS eastonite probably depend on the bulk composition and the nature of the Ti-saturating phase, respectively.

Titanite rims are most commonly seen in rocks in which the QBS veins occur; these also have the high-Ti eastonite. Thus, titanite formation appears to be linked to these veins in some way. The formation of titanite from ilmenite or rutile requires the addition of Ca and Si. We suggest that titanite growth occurred during metamorphism in the altered rocks around the QBS veins owing to elevated Ca and Si (now manifested as calcic plagioclase and quartz) that originally resulted from hydrothermal activity.

Amphibole

Amphibole with a preferred orientation, the metamorphic amphibole, is typically finer grained than most of the other varieties of amphibole and exhibits a wide range of composition (Fig. 5a), which is taken to reflect protolith composition. That the metamorphic amphibole is genetically distinct from most of the other amphibole varieties is supported by the amphibole – chlorite and amphibole – biotite relationships (Figs. 10, 11), as well as their textures. In both cases, all metamorphic pairs can be described by a single K_D value, CAA for chlorite – amphibole and BAA for biotite – amphibole (Table 6), indicating a consistent relationship among chlorite, biotite and amphibole.

The dark green cores of zoned crystals and the dark green relict crystals (magnesiohornblende and tschermakite; Figs. 5b, c) within massive alteration-induced amphibole are defined by the same K_D values as the metamorphic amphibole crystals. This is true for both chlorite – amphibole and biotite – amphibole pairs (Groups CAA and BAA, Figs. 10 and 11, Table 6) and indicates that metamorphic and relict amphibole and the cores of zoned crystals all formed under similar conditions, and probably during, or soon after, deformation. Such a conclusion is consistent with the textural evidence that these types formed prior to the alteration amphiboles.

The randomly oriented porphyroblasts are generally coarser grained than the metamorphic amphibole and must have postdated the formation of the penetrative fabric. They form a compositionally bimodal population (Fig. 5a). One group contains magnesiohornblende and actinolite, and is similar to vein, alteration and patchy amphibole (Figs. 5c, d). The second group contains ferrotschermakite similar to the more iron- and aluminum-rich metamorphic amphibole. The magnesiohornblende – actinolite group of random amphibole is characterized by $K_D^{chl/amp}$ and $K_D^{bt/amp}$ values that place it in Groups CAB and BAB (Figs. 10 and 11, Table 6) along with alteration and patchy amphibole. Although it may belong to Groups CAB and BAB, the random ferrotschermakite group has K_D values with chlorite and biotite that are closer to those for the rims of zoned amphibole crystals and the vug and vug-related amphibole (Groups CAC and BAC, Figs. 10 and 11, Table 6). The split of the random amphibole into two populations presumably indicates that these porphyroblasts are related to two different events, one associated with the formation of the vugs and the other with the patchy and alteration amphibole.

Most vein and alteration amphiboles have a more restricted compositional range than the other types (Fig. 5d), and both define the same population of K_D values with respect to chlorite and biotite (CAB and BAB; Figs. 10, 11). The patchy amphiboles have similar compositions to the alteration amphiboles (Figs. 5c, d) and are defined by the same K_D with respect to biotite, indicating that they were formed during the same event. It would be reasonable to propose that the composition of these amphibole types was controlled by fluid rather than rock chemistry, a proposal that is supported by the more restricted compositions and distinctive K_D values. However, it is clear that there is a consistent relationship between the composition of the amphibole and the minerals being replaced, namely chlorite and biotite (Figs. 10, 11). This leads to the inference that host-rock composition played a role in controlling the composition of the alteration amphiboles. The random amphiboles that fall within the BAB group were presumably formed by the same alteration event that formed the more massive alteration.

Vug and vug-related amphiboles define intermediate populations with respect to both chlorite (CAC) and biotite (BAC). In the case of chlorite, this group also includes rims on zoned crystals. These relationships suggest that the vug amphiboles represent an event different from that which formed the alteration and patchy amphibole. Of all the groups, the composition of vug amphibole shows the least scatter (Fig. 11), which may reflect higher water:rock ratios and less influence from host-rock composition. Nevertheless, there is still a relationship to the composition of precursor biotite (Fig. 11), and the distinct K_D values (groups CAC and BAC) indicate a distinct event. Further, it would appear that some of the random amphiboles formed during this event.

Conclusions

1. Amphiboles in the MacLellan deposit are represented by a wide variety of textural types. These include metamorphic porphyroblasts, randomly oriented, postmetamorphic porphyroblasts and aggregates, amphiboles related to quartz – chlorite – biotite vugs, and aggregates of massive amphibole in alteration haloes around veins.

2. These amphiboles are all calcic, but represent a wide compositional range, including ferrotschermakite, tschermakite, magnesiohornblende and actinolite.

3. Distribution of Fe and Mg among amphibole, biotite and chlorite (K_D values) indicate three amphibole-forming events. These represent 1) metamorphism, 2) the main episode of quartz–amphibole vein formation and alteration, and 3) an event that formed the vugs. The randomly oriented porphyroblasts and aggregates appear to be associated with both the main alteration event and the vug-forming event, which is consistent with their formation after the main episode of metamorphism and deformation.

4. A correlation between the composition of alteration-induced amphiboles associated with veins and the composition of protolith chlorite and biotite indicates

that the protolith's composition has strongly influenced the composition of the fluid–rock system, and that alteration occurred under low fluid:rock ratios.

5. Metamorphic biotite is Mg-rich, with X_{Mg} ranging from 0.53 to 0.77.

6. The composition of biotite in and around metamorphosed quartz – biotite – sulfide (QBS) veins is more restricted than that of the host-rock biotite, and may represent that of a fluid-buffered protolith.

7. Ti contents in biotite correlate with the nature of the associated Ti-oxide phase, increasing from rutile to ilmenite ± rutile to titanite – ilmenite ± rutile. The QBS-associated biotite typically has a high Ti content and is associated with titanite. This trend is attributed to premetamorphic metasomatism related to the QBS vein-forming event.

Acknowledgements

The authors thank LynnGold (formerly Sherrgold) Resources for access to the MacLellan mine and to drill core, and for financial assistance. We also thank the Manitoba Department of Energy and Mines for logistical and financial support, and in particular to Dr. M. Fedikow. Thanks go to Carl Henderson for his assistance with the electron-microprobe analyses. The manuscript was improved by comments made by A.E. Williams-Jones, Robert F. Martin, Charles Guidotti and David Lentz. This research was supported in part by an NSERC operating grant to I.M.S.

References

BLACKBURN, W.H. (1968): The spatial extent of chemical equilibrium in some high-grade metamorphic rocks from the Grenville of southeastern Ontario. *Contrib. Mineral. Petrol.* **19**, 72-92.

BLUNDY, J.D. & HOLLAND, T.J.B. (1990): Calcic amphibole equilibria and a new amphibole – plagioclase geothermometer. *Contrib. Mineral. Petrol.* **104**, 208-224.

CASTRO, A. & STEPHENS, W.E. (1992): Amphibole-rich polycrystalline clots in calc-alkaline granitic rocks and their enclaves. *Can. Mineral.* **30**, 1093-1112.

CLOWE, C.A., POPP, R.K. & FRITZ, S.J. (1988): Experimental investigation of the effect of oxygen fugacity on the ferric–ferrous ratios and unit-cell parameters of four natural clinoamphiboles. *Am. Mineral.* **73**, 487-499.

COSCA, M.A., ESSENE, E.J. & BOWMAN, J.R. (1991): Complete chemical analysis of metamorphic hornblendes: implications for normalizations, calculated H_2O activities, and thermobarometry. *Contrib. Mineral. Petrol.* **108**, 472-484.

DEER, W.A, HOWIE, R.A. & ZUSSMAN, J. (1992): *An Introduction to the Rock-Forming Minerals* (second ed.). Longman, London, U.K.

DYAR, M.D. (1990): Mössbauer spectra of biotite from metapelites. *Am. Mineral.* **75**, 656-666.

________, GUIDOTTI, C.V., HARPER, G.D., MCKIBBEN, M.A. & SACCOCIA, P.J. (1992): Controls on ferric iron in chlorite. *Geol. Soc. Am., Abstr. Programs* **24**(7), A130.

DYMEK, R.F. (1983): Titanium, aluminum and interlayer cation substitutions in biotite from high-grade gneisses, West Greenland. *Am. Mineral.* **68**, 880-899.

EUGSTER, H.P. & SKIPPEN, G.B. (1967): Igneous and metamorphic reactions involving gas equilibria. *In* Researches in Geochemistry **2** (P.H. Abelson, ed.). John Wiley & Sons, New York, N.Y. (492- 520).

FEDIKOW, M.A.F. (1986): Geology of the Agassiz (MacLellan) stratabound Au–Ag deposit, Lynn Lake, Manitoba. *Manitoba Energy and Mines, Geological Services Branch, Open File Rep.* **OF85-5**.

________ (1992): Rock geochemical alteration studies at the MacLellan Au–Ag deposit, Lynn Lake, Manitoba. *Manitoba Energy and Mines, Econ. Geol. Rep.* **ER92-1**.

________, PARBERY, D. & FERREIRA, K.J. (1991): Geochemical target selection along the Agassiz metallotect utilizing stepwise discriminant analysis. *Econ. Geol.* **86**, 588-599.

GAGNON, J. (1991): *Geology, Geochemistry and Genesis of the Proterozoic MacLellan Au–Ag Deposit, Lynn Lake Greenstone Belt, Manitoba.* M.Sc. thesis, Univ. of Windsor, Windsor, Ontario.

GILBERT, H.P., SYME, E.C., ZWANZIG, H.V. & HERMAN, V. (1980): Geology of the metavolcanic and volcaniclastic metasedimentary rocks in the Lynn Lake area. *Manitoba Energy and Mines, Geol. Pap.* **GP80-1**.

GUIDOTTI, C.V. (1984): Micas in metamorphic rocks. *In* Micas (S.W. Bailey, ed.). *Rev. Mineral.* **13**, 357-467.

________, CHENEY, J.T & GUGGENHEIM, S. (1977): Distribution of titanium between coexisting muscovite and biotite in pelitic schists from northwestern Maine. *Am. Mineral.* **62**, 438-448.

________ & DYAR, M.D. (1991): Ferric iron in metamorphic biotite and its petrologic and crystallochemical implications. *Am. Mineral.* **76**, 161-175.

HAWTHORNE, F.C. (1983): The crystal chemistry of the amphiboles. *Can. Mineral.* **21**, 173-480.

HOLDAWAY, M.J., DUTROW, B.L. & HINTON, R.W. (1988): Devonian and Carboniferous metamorphism in west-central Maine: the muscovite–almandine geobarometer and the staurolite problem revisited. *Am. Mineral.* **73**, 20-47.

________, MUKHOPADHYAY, B., DYAR, M.D., GUIDOTTI, C.V. & DUTROW, B.L. (1997): Garnet–biotite geothermometry revised: new Margules parameters and a natural specimen dataset from Maine. *Am. Mineral.* **82**, 582-595.

KONTAK, D.J. & SMITH, P.K. (1993): A metaturbidite-hosted lode gold deposit: the Beaver Dam deposit, Nova Scotia. I. Vein paragenesis and mineral chemistry. *Can. Mineral.* **31**, 471-522.

KRETZ, R. (1959): Chemical study of garnet, biotite, and hornblende from gneisses of southwestern Quebec, with emphasis on the distribution of elements in coexisting minerals. *J. Geol.* **67**, 371-402.

________ (1978): Distribution of Mg, Fe^{2+} and Mn in some calcic pyroxene – hornblende – biotite – garnet gneisses and amphibolites from the Grenville Province. *J. Geol.* **86**, 599-619.

________ (1983): Symbols for rock-forming minerals. *Am. Mineral.* **68**, 277-279.

LABOTKA, T.C. (1983): Analysis of the compositional variations of biotite in pelititc hornfelses from northeastern Minnesota. *Am. Mineral.* **68**, 900-914.

LEAKE, B.E., and 21 others (1997): Nomenclature of amphiboles: report of the Subcommitee on Amphiboles of the International Mineralogical Association, Commission on New Minerals and Mineral Names. *Can. Mineral.* **35**, 219-246.

MUNOZ, J.L. & SWENSON, A. (1981): Chloride–hydroxyl exchange in biotite and estimation of HCl/HF activities in hydrothermal fluids. *Econ. Geol.* **76**, 2212-2221.

NELSON, D.O. & GUGGENHEIM, S. (1993): Inferred limitations to the oxidation of Fe in chlorite: a high temperature single-crystal X-ray study. *Am. Mineral.* **78**, 1197-1207.

POUCHOU, J.-L. & PICHOIR, F. (1984): A new model for quantification of X-ray analysis. I. Application to the analysis of homogeneous samples. *Recherche Aérospatiale* **3**, 13-36.

RANCOURT, D.G., DANG, M.-Z. & LALONDE, A.E. (1992): Mössbauer spectroscopy of tetrahedral Fe^{3+} in trioctahedral micas. *Am. Mineral.* **77**, 34-43.

REBBERT, C.R., PARTIN, E. & HEWITT, D.A. (1995): Synthetic biotite oxidation under hydrothermal conditions. *Am. Mineral.* **80**, 345-354.

RIEDER, M., and 14 others (1998): Nomenclature of the micas. *Can. Mineral.* **36**, 905-912.

ROBINSON, P., SPEAR, F.S., SCHUMACHER, C., LAIRD, J., KLEIN, C., EVANS, B.W. & DOOLAN, B.L. (1982): Phase relations of metamorphic amphiboles: natural occurrence and theory. *In* Amphiboles: Petrology and Experimental Phase Relations (D.R. Veblen & P.H. Ribbe, eds.). *Rev. Mineral.* **9B**, 1-227.

SAMSON, I.M. & GAGNON, J.G. (1995): Episodic fluid infiltration and the genesis of the Proterozoic MacLellan Au–Ag deposit, Lynn Lake greenstone belt, Manitoba. *Explor. Mining Geol.* **4**, 33-50.

SCHUMACHER, J.C. (1997): The estimation of the proportion of ferric iron in the electron-microprobe analysis of amphiboles. *Can. Mineral.* **35**, 238-246.

SPEAR, F. (1981): An experimental study of hornblende stability and compositional variability in amphibolite. *Am. J. Sci.* **281**, 697-734.

________ & KIMBALL, K.L. (1984): RECAMP – a FORTRAN IV program for estimating Fe^{3+} contents in amphiboles. *Comput. Geosci.* **10**, 317-325.

TANER, M.F., TRUDEL, P. & PERRAULT, G. (1986): Géochimie de la biotite associée à certains gisements d'or de Val d'Or, Malartic et Chibougamau, Québec. *Can. Mineral.* **24**, 761-774.

WILLIAMS, M.L. & GRAMBLING, J.A. (1990): Manganese, ferric iron, and the equilibrium between garnet and biotite. *Am. Mineral.* **75**, 886-908.

ZHU, CHEN & SVERJENSKY, D.A. (1991): F–Cl–OH partitioning between biotite and apatite. *Geochim. Cosmochim. Acta* **56**, 3435-3467.

Received January 28, 1998, revised manuscript accepted October 10, 1999.